Chemical Engineering Science, 1977, Vol. 32, pp. 109–117. Pergamon Press. Printed in Great Britain

ON THE TRANSITION FROM A FIXED TO A SPOUTED BED

J. A. ASENJO,† R. MUÑOZ and D. L. PYLE‡

Departmento de Tecnología Química, Universidad de Chile, Beauchef 861, Santiago, Chile

(*Received* 11 *March* 1976; *accepted* 24 *May* 1976)

Abstract—Theory is developed to predict the maximum pressure drop and superficial gas velocity during the onset of spouting. The theory, which is valid for low Reynolds number flows, assumes an approximate form for the gas distribution in the bed from the central injection point. Spouting is predicted to commence when the upwards drag force exerted by the gas balances the weight of particles within the volume enclosed by the gas flow. There is reasonable agreement between the theory and experimental results for the transition and some experimental results for pressure distributions in situations not covered by the theory are presented. In particular, the existence and importance of radial pressure gradients near the injection point are discussed.

INTRODUCTION

The expression "spouted bed" refers to a bed of particles through which a vertical rising jet is injected from the centre of the base. When the steady stage is reached, a circulation pattern is established in which the solids are entrained upwards by the fast central jet ("spout"), rise above the level of the bed surface and subsequently fall outwards to the annulus surrounding the spout, where a slow downwards bulk motion completes the cycle. Since their introduction by Mathur and Gishler[1], spouted beds have become accepted in many situations as a better alternative to fluidisation for the handling of coarse particles. Comprehensive reviews of their behaviour and application have recently been published by Mathur[2] and by Mathur and Epstein[3, 4].

The present investigation is concerned with the onset of spouting. This is an important factor in design, for experiments have shown that a peak pressure drop across the bed is reached for a gas flow just below the stage of incipient spouting. The same feature is exhibited by fluidised beds, but whereas in the latter case the maximum pressure drop does not exceed the steady state value by more than a few percent, in spouted beds the excess may be one or two orders of magnitude higher.

Measurements as well as visual qualitative observations in half-cylindrical beds (Mathur and Gishler[1]; Madonna and Lama[5]; Malek and Lu[6]) and in two-dimensional beds (Volpicelli and Raso[7]) have given a clear picture of the development of a spout, as outlined in Fig. 1. For low velocities, the pressure drop ΔP increases proportionately to the superficial velocity U raised to some power between one and two, the upper and lower limits corresponding to the low or high Reynolds number regimes for flow through a packed bed. At some point B', a small cavity is formed around the inlet (the internal spout); ΔP keeps increasing but at a lower rate, up to a maximum ΔP_m at point B with velocity U_m; from then on, as the internal spout develops and reaches the bed surface, ΔP falls very quickly to point C, in whose neighbourhood it stabilises for larger flows (D). As the flow is decreased, a hysteresis loop is usually present, C–E–F–O, with lower pressure drops for the same velocity than in the ascending branch. The point E, being the most reproducible, is customarily taken as the definition of minimum spouting and of the minimum spouting velocity U_{ms}.

In the same way as is done for incipient fluidisation, the condition of incipient spouting can be conceived in general terms as resulting from equilibrium between the upward drag force exerted by the fluid on the particles and the buoyant weight of the bed. Such an equation has led to a number of semi-empirical formulae which relate ΔP_m to either the corresponding uniform packed bed pressure drop (Madonna and Lama[5]) or the bed weight (Malek and Lu[6]; Manurung[8]) through some empirical coefficient. It can be readily seen, however, that the localized nature of the fluid jet as it emerges into a bed of particles at rest must strongly affect the evaluation of both the upward drag force of the fluid and the solids resistance. For one thing the fluid velocities near the inlet are many times larger than the average across the bed, which means that the particles in that region are subject to very large drag forces. On the other hand, this concentrated force is resisted by the whole of the bed in a way that should be evaluated in terms of the rheological properties of granular masses. Most likely, there are regions along the bottom corners of the bed which contribute nothing to either term in the condition of near equilibrium.

In regard to the minimum spouting velocity U_{ms}, Mathur and Epstein[4] list thirteen different empirical correlations which have been proposed in the past. According to their review, the best agreement with published laboratory experiments is still given by the original formula of Mathur and Gishler[1]; however, as they remark, even this expression is not suitable for extrapolation to larger sizes since it predicts continually decreasing values of U_{ms} for increasing sizes of geometrically similar beds, which leads eventually to an unrealistic prediction.

†Present address: Dept. of Chemical Engineering, University College, London WC1, England.

‡Present address: Dept. of Chemical Engineering, Imperial College, London SW7, England.

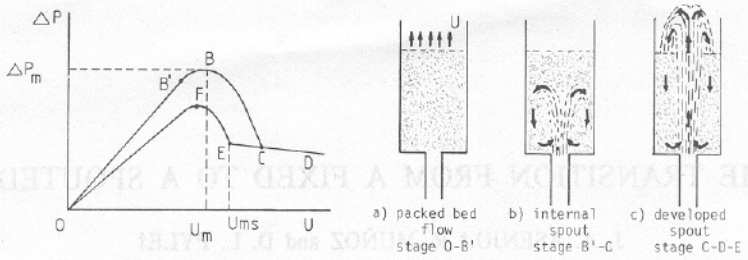

Fig. 1. Schematic diagram of pressure drop vs superficial velocity in the development of a spout.

Therefore, an attempt has been made in the present study to derive analytical expressions for the two basic variables ΔP_m and U_m. A simplified model is postulated, namely, that a laminar flow distribution develops from the injection point across the bed. This condition is maintained up to the stage of maximum pressure drop, at which point the total fluid drag on the particles within a central core balances their buoyant weight, this equilibrium condition inducing the onset of spouting. Such an analysis does not lead to the determination of U_{ms} (see Fig. 1); the available experimental evidence indicates that U_m and U_{ms} are not too far apart in practice (U_{ms} being up to 25% greater than U_m), so that the former can be taken as a first estimate of the latter.

THEORY

The flow of an incompressible fluid through a uniform packed bed of particles is governed by[9]:

$$\nabla P = A\underline{U} + B|\underline{U}|\underline{U}. \tag{1}$$

For uniform one-dimensional flows this reduces to Ergun's equation. For Reynolds numbers less than about 10, that is, under laminar flow conditions, in a homogeneous packed bed the components of the pressure gradient ∇P and superficial velocity $\underline{U}$ are related by the first term in eqn (1). Using the coefficient from Ergun's equation we thus have:

$$\nabla P = -\frac{150\mu(1-\epsilon)^2}{D_p^2\epsilon^3}\underline{U}. \tag{2}$$

The subsequent theory is developed for this case of low Reynolds number flows; some aspects of higher Reynolds number flows are discussed later.

Assuming that at low velocities the gas flow is incompressible and that the voidage fraction remains constant, for steady flows the equation of continuity is:

$$\nabla \cdot \underline{U} = 0. \tag{3}$$

Thus taking the divergence of (2), it is seen that the pressure distribution is governed by Laplace's equation:

$$\nabla^2 P = 0. \tag{4}$$

The linearity of eqns (2) and (4) can be readily exploited, as indeed has been the case in the analysis of bubbling fluidised beds. In order to describe the gas flow distribution at low Reynolds numbers and under the conditions of Fig. 1(a) it is necessary to solve eqn (4) together with the appropriate boundary conditions. Rather than seek a numerical solution, we consider here an approximate analytic solution to the problem.

As Scheidegger[9] points out, eqn (2) implies that, provided ϵ is independent of position, the velocity $\underline{U}$ is irrotational, despite the fact that we are dealing with a low Reynolds number flow. We can thus define a velocity potential ϕ proportional to the pressure and which will also satisfy Laplace's equation. The application of this approach in the treatment of seepage problems through porous media is also discussed in some detail by Scheidegger[9]. Thus, defining a velocity potential by:

$$\phi = -\frac{D_p^2}{150\mu}\frac{\epsilon^3}{(1-\epsilon)^2}P \tag{5}$$

eqn (2) may be written

$$\underline{U} = \nabla\phi. \tag{6}$$

A flow which approximately satisfies the boundary conditions is the axisymmetric irrotational flow resulting from a source of strength Λ in a parallel flow which has uniform velocity U as $x \to \infty$. The column is assumed to be defined by the stream line with stream function ψ_c shown in Fig. 2. The source is located somewhere below the base of the column; this point defines the origin of the

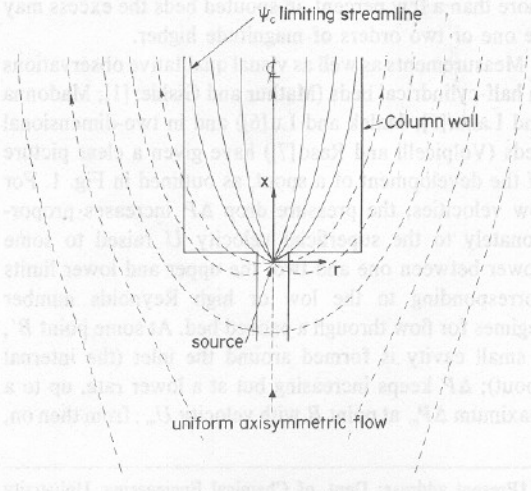

Fig. 2. Location of the axisymmetric irrotational flow model with respect to the spouting column.

coordinate system. Thus the flow is described by[10]:

$$\psi = \frac{1}{2} Ur^2 + \frac{\Lambda}{4\pi}\left(1 - \frac{1}{\sqrt{\left(1+\frac{r^2}{x^2}\right)}}\right). \quad (7)$$

The velocity potential corresponding to (7) is:

$$\phi = Ux - \frac{\Lambda}{4\pi\sqrt{(x^2+r^2)}}. \quad (8)$$

As $x \to \infty$ it is assumed that the limiting stream line (ψ_c) coincides with the column, so that as $x_c \to \infty$, $r_c \to R$. Thus we can write, for any coordinates (x_c, r_c) on the limiting streamline:

$$\psi_c = \frac{1}{2} UR^2 = \frac{1}{2} Ur_c^2 + \frac{\Lambda}{4\pi}\left(1 - \frac{1}{\sqrt{\left(1+\frac{r_c^2}{x_c^2}\right)}}\right). \quad (9)$$

The analysis will be restricted to the core region inside the limiting streamline and we assume that there is no gas flow in the broken line area indicated on Fig. 2.

Defining $K = \pi R^2 U/\Lambda$ as the fraction of the source flow Λ that passes through the column, we can solve for x_c from eqn (9) in terms of dimensionless coordinates $\xi = x/R$, $\rho = r/R$:

$$\xi_c = \frac{\rho_c\left(\frac{1-2K}{2K} + \rho_c^2\right)}{\sqrt{\left((1-\rho_c^2)\left(\frac{1-K}{K} + \rho_c^2\right)\right)}}. \quad (10)$$

Solving from eqns (5), (8) and (10), the pressure distribution along ψ_c is given by:

$$P_c = -\frac{150\mu}{D_p}\frac{R}{D_p}\frac{(1-\epsilon)^2}{\epsilon^3}\frac{(K-1+2\rho_c^2-4K\rho_c^3+3K\rho_c^4)U}{2K\rho_c\sqrt{\left[(1-\rho_c^2)\left(\frac{1-K}{K}+\rho_c^2\right)\right]}}. \quad (11)$$

Inception of the spout

On the basis of the model of the gas flow we can attempt to predict the inception of spouting by establishing the conditions under which the upwards drag force F_x from the gas on the particles just balances the weight of particles, W_c, within the core volume contained between the top and bottom of the bed and bounded by the limiting streamline. Thus:

$$F_x + W_c = 0. \quad (12)$$

This condition is, of course, analogous to that used to determine the point of incipient fluidisation over a uniformly fluidised bed, the main difference being that in the present work the gas velocity distribution is not uniform, and the balance expressed by eqn (12) applies only to a fraction (of volume V_c, say,) of the total bed volume.

Considering the drag forces acting over a small volume of bed which is large relative to the particle size so that the drag force remains continuous and assuming that inertial forces may be neglected, then:

$$\underline{f} = -\nabla P = \frac{150\mu(1-\epsilon)^2}{D_p^2\epsilon^3}\underline{U}. \quad (13)$$

The total drag force over the core volume V_c can be obtained by integrating (13) over the core. In the case of the axisymmetric problem under consideration, the tangential component of the drag force must be zero by symmetry as must the integral over the region of the radial component. The total drag force over the region in question can thus be derived by integrating the axial component of eqn (13) over the volume V_c, i.e.

$$F_x = \frac{150\mu}{D_p^2}\frac{(1-\epsilon)^2}{\epsilon^3}\int_{V_c} \underline{U}\cdot\underline{x}\,\mathrm{d}V \quad (14)$$

where $\underline{U}\cdot\underline{x} = U_x$ is the x-component of the fluid velocity. Transforming into cylindrical coordinates such that $\mathrm{d}V = 2\pi r\,\mathrm{d}r\,\mathrm{d}x$, and noting that $\int_0^{r_c} U_x 2\pi r\,\mathrm{d}r = Q = \pi UR^2$ (= the volumetric gas flow-rate), eqn (14) becomes:

$$F_x = \frac{150\mu}{D_p^2}\frac{(1-\epsilon)^2}{\epsilon^3}\int_{x_i}^{x_i+H} \pi UR^2\,\mathrm{d}x \quad (15)$$

$$= 150\pi\mu\frac{(1-\epsilon)^2}{\epsilon^3}\left(\frac{R}{D_p}\right)^2 HU \quad (16)$$

where x_i is the axial coordinate at the base of the bed, and H is the total bed height.

It will be seen that the drag force is the same as that for uniform flow across a packed bed of uniform cross-sectional area πR^2 and of height H.

The weight of particles contained within the volume under consideration can be obtained by integration since

$$V_c = \pi\int_{x_i}^{x_H} r_c^2\,\mathrm{d}x = \pi R^3\int_{\xi_i}^{\xi_H}\rho_c^2\,\mathrm{d}\xi. \quad (17)$$

Without significant loss of accuracy in the present calculations (see Fig. 3), we can set $x_i = 0$, so that the weight of bed contained within the limiting streamline ψ_c is:

$$W_c = -(1-\epsilon)\rho_p g\pi R^3\int_0^{\xi_H}\rho_c^2\,\mathrm{d}\xi \quad (18)$$

where ρ_c and ξ are related through eqn (10).

Equation (18) can be integrated (Asenjo[11]) to give

$$W_c = -(1-\epsilon)\rho_p g\pi R^2 H\beta(K, H/R) \quad (19)$$

where the dimensionless β is given by:

$$\frac{H\beta}{R} = \frac{(1-2K)E(\theta,\Omega) - (1-K)F(\theta,\Omega)}{3K\sqrt{K}} + \frac{2\rho_H + \rho_H^3(1-2K) + 2K\rho_H^5}{6K\sqrt{\left[(1-\rho_H^2)\left(\frac{1-K}{K}+\rho_H^2\right)\right]}} \quad (20)$$

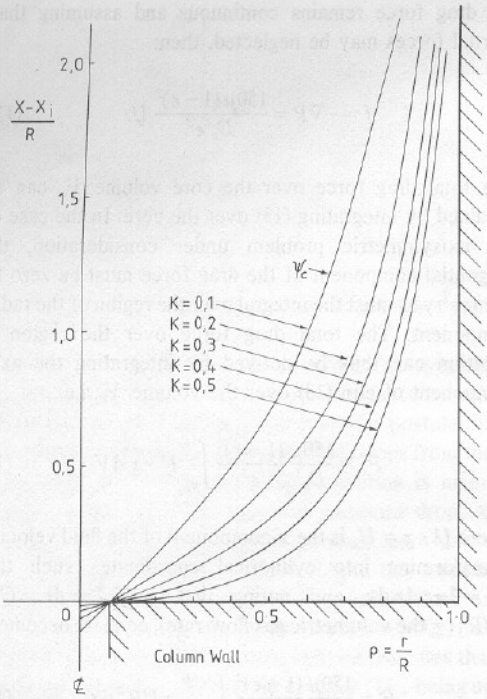

Fig. 3. Shape of the limiting streamline ψ_c for various positions of the source with respect to the column base, i.e. various values of K.

in which $F(\theta, \Omega)$ and $E(\theta, \Omega)$ are elliptic integrals of the 1st and 2nd kinds respectively; also

$$\theta = \sin^{-1}\sqrt{K}$$

$$\Omega = \sin^{-1}\frac{\rho_H}{\sqrt{(1-K+K\rho_H^2)}}.$$

For constant r_i/R, ρ_H is a function only of $(K, H/R)$ and so the same is true of β, which is plotted from eqn (20) in Fig. 4; for small K, and large H/R, $\beta \to 1$, as would be expected. Setting $F_x = -W_c$ (i.e. eqn 12), from eqns (16), (19) and (20) the superficial velocity at the point of inception of spouting is:

$$U_m = \frac{\rho_p g D_p^2 \epsilon^3}{150\mu(1-\epsilon)}\beta(K, H/R). \quad (21)$$

It will be noted that the group of parameters of multiplying β corresponds to the minimum fluidisation velocity U_{mf} for the same system, on the assumption that $\epsilon = \epsilon_{mf}$, i.e.

$$U_m = U_{mf}\beta(K, H/R). \quad (22)$$

We note also that the weight of particles contained within the core region is related to the total weight of particles in the bed by

$$W_c = \beta W_{\text{total}}. \quad (23)$$

Referring to Fig. 2 it is seen that the equipotential surfaces in this model are not plane, expecially so in the

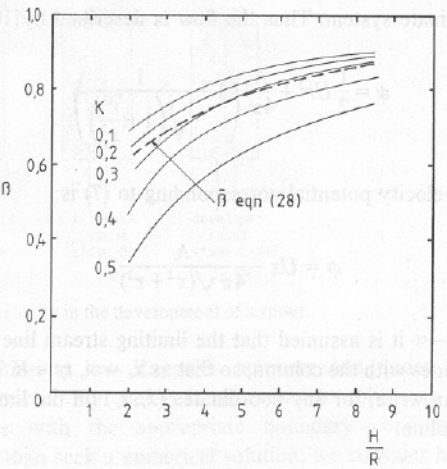

Fig. 4. Approximate expression for average β for the range $0.1 \leq K \leq 0.5$.

region of the base of the column. Therefore, we assume that the overall pressure drop can be defined as the difference between the pressure on the limiting streamline at the edge of the inlet orifice (subscript i) and the pressure at the centreline on top of the bed (subscript H). Thus, from eqns (5), (8) and (11):

$$\Delta P = P_i - P_H = \frac{150\mu}{D_p^2}\frac{(1-\epsilon)^2}{\epsilon^3}HU\eta(K, H/R) \quad (24)$$

where the dimensionless parameter η is given by[11]:

$$\eta = 1 - \frac{R}{4KH}\left(\frac{1}{\frac{H}{R} + \frac{\rho_i(1-2K+2K\rho_i^2)}{2\sqrt{[K(1-\rho_i^2)(1-K+\rho_i^2)]}}} - \frac{1}{\rho_i\sqrt{\left[1+\frac{(1-2K+2K\rho_i^2)^2}{4K(1-\rho_i^2)(1-K+\rho_i^2)}\right]}}\right). \quad (25)$$

As was the case for β, η is only a function of $(K, H/R)$ for constant r_i/R.

It is assumed in this model that the maximum pressure drop occurs at the point of equilibrium between F_x and $-W_c$, since once the spout is fully formed there is a sharp fall in pressure loss. Under the conditions of maximum pressure drop, then, $U = U_m$, and substituting from (21) into (24) we find:

$$\Delta P_m = (1-\epsilon)\rho_p g H\beta\eta. \quad (26)$$

Under conditions of uniform fluidisation the pressure drop, ΔP_f, is equal to $(1-\epsilon)\rho_p g H$ so that:

$$\Delta P_m = \Delta P_f \beta\eta. \quad (27)$$

Approximate forms for β, η

In the proposed model the value of K (the fraction of the source flow passing through the column) is unknown, and would have to be determined experimentally. However, it is clear that $0 < K \leq 0.5$, where the upper limit corresponds to the situation where the source is

located in the plane of the column base. The position of the source with respect to the column base as a function of K is shown in Fig. 3, where the form of the penetrating jet is plotted for various values of K; as $K \to 0.5$ the vertical velocity component of the spout at entry to the bed tends to zero, which is clearly physically unrealistic. Similarly, values of K close to zero may be ruled out on physical grounds since the fluid would only fill a significant proportion of the bed cross-section at very high values of bed height. In Fig. 4, values of β are shown as a function of K in the region $0.1 < K < 0.5$. Since the value of K is unknown, as a first approximation it was decided to use an average value of β. K may also be a function of r_i/R, but in the absence of any experimental information we consider here only its dependence on H/R. The following expression for β to be used in eqn (21) is also shown in Fig. 4:

$$\bar{\beta} = 1 - 0.55\,e^{-0.18H/R}. \tag{28}$$

The maximum deviation from this value (at high values of K, and low H/R_c) would be around 50%; for lower K and higher H/R_c the deviation is around ±15%.

A similar reasoning leads to the following expression for an average value of $\beta\eta$ to be used in eqns (26) and (27):

$$\overline{\beta\eta} = 1 + 2.8\,e^{-0.156H/R}. \tag{29}$$

This expression is compared with the computed values of $\beta\eta$ in Fig. 5. The deviation from the average value ranges from around ±15% to around ±30% at high H/R_c.

Thus the superficial velocity and pressure drop at the point of inception of spouting should be given to within the same limits of accuracy by, respectively:

$$U_m = U_{mf}(1 - 0.55\,e^{-0.18H/R}) \tag{30}$$

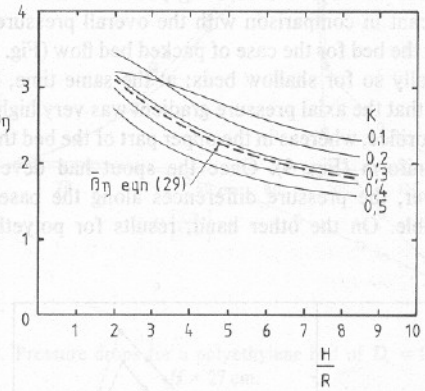

Fig. 5. Approximate expression for average $\beta\eta$ for the range $0.1 \leq K \leq 0.5$.

and

$$\Delta P_m = \Delta P_f(1 + 2.8\,e^{-0.156H/R}). \tag{31}$$

There are two features of eqn (30) that are worth noting. Firstly, as H tends to the maximum spoutable bed depth H_{max}, U_m tends to become equal to U_{mf}; experimental results given by Lefroy and Davidson[12] and shown by Mathur and Epstein[4] in the case of sand certainly show that U_{ms} tends to U_{mf} under these conditions; for instance, in the present study typical values of H_{max}/R were of the order of 12, corresponding to a difference of only 6% between U_m and U_{mf}. In the second place, for geometrically similar beds (H/R = const), eqn (30) predicts a constant value of U_m; this seems to be in better agreement with the probable trend of experimental data than the behaviour of other correlations, as pointed out in the Introduction.

EXPERIMENTAL

Experiments were carried out in two cylindrical flat-based beds of internal diameter 14.2 and 8.7 cm; the air was introduced through an orifice centrally located in the column base. The orifice diameter was 1.1 cm for the larger column and 0.6 cm for the smaller one. The injection point was covered with a wire screen to prevent particles falling back into the air supply system.

The characteristics of the three types of particle used are given in Table 1, which also lists the range of Reynolds numbers based on the average superficial velocity for the conditions of the experiments.

The air flowrate was measured by means of an orifice plate calibrated *in situ*; superficial air velocities in the range 10–150 cm/sec were possible.

The pressure distribution within the bed was measured by means of a 6 mm o.d. tube with 1 mm pressure tappings at 39 mm from the end of the tube, introduced from the top of the bed. Two pressure measuring points were located in the base of the larger column at 1.3 and 6.1 cm from the centreline.

The measurements of pressure distribution and overall pressure loss were extremely sensitive to the values of the voidage fraction (as is expected from Ergun's equation). This has a considerable effect on both the pressure drop curves and also the calculated value of the fluidising velocity (U_{mf}). In each case in calculating the value of U_{mf} it is assumed that $\epsilon = \epsilon_{mf}$, although in fact there is strictly only one value of both ϵ_{mf} and the corresponding U_{mf}. Thus great care was taken in these measurements, and beds of sand with different porosities (which depended on the initial compaction) were used in these studies.

Table 1. Characteristics of particles used in the experiments

Particle	Mean size D_p cm	Density ρ g/cm^3	Voidage fraction ϵ	Reynolds number Re
Sand	0.061	2.66	0.40 – 0.43	9–22
Wheat	0.38	1.35	0.40	180–470
Polyethylene chips	0.34	0.903	0.40	150–370

RESULTS

In relation to the onset of spouting as depicted in Fig. 1, broadly three different types of behaviour were observed, and found to depend on the bed height. For very shallow beds the transition between a packed bed and spouting was found to be very short-lived, since a small increase in gas velocity produced a very large decrease in pressure drop. In these beds the spout formed was stable except at the highest velocities. For beds with height around one-half the maximum, an internal spout was formed during the transition from packed bed to spouting with some bubbling at the top of the column. The fully-developed spout was again stable for all but the highest velocities. Under the latter conditions violent instability was observed and found to be especially sensitive to the alignment to the vertical of the air inlet. Beds with height around the maximum for which spouting was possible had both an internal spout and significant bubbling in the transition regime. In fact, for these highest beds it was impossible to achieve spouting except by first exceeding the minimum spouting velocity and then gradually reducing the gas velocity.

Values of the spouting velocity, U_{ms}, are compared with the well-tried correlation of Mathur and Gishler in Fig. 6.

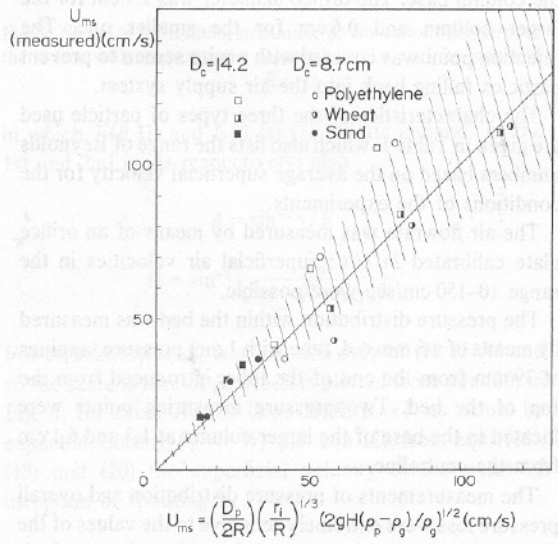

Fig. 6. Measured values of minimum spouting velocity compared with the correlation of Mathur and Gishler [1].

The hatched zone represents the spread of points used by Mathur and Fishler in developing the correlation. There is fair agreement between our experiments and their correlation.

With respect to the measurement of the overall pressure drop, a problem arose because it proved impossible to measure the inlet pressure P_i (see Fig. 7) in

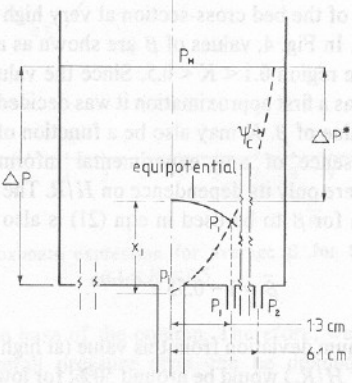

Fig. 7. Definition of pressure measurements.

view of the pressure drop across the screen at the entry to the bed. In practice the closest measuring point (1) to the air inlet was located at 1.3 cm from the centreline along the base of the bed. It is generally assumed that radial pressure gradients in spouting beds can be ignored, and there is indeed a degree of ambiguity in the studies of pressure drops over spouted beds that are reported in the literature with respect to the location of the measuring point. In fact, measurements showed that at least in the phase before the spout had developed radial pressure gradients along the base of the bed were very pronounced.

With sand particles, the difference between the pressures at the two measuring points on the base was significant in comparison with the overall pressure drop across the bed for the case of packed bed flow (Fig. 8) and especially so for shallow beds; at the same time, it was found that the axial pressure gradient was very high close to the orifice, whereas in the upper part of the bed the flow was uniform (Fig. 9). Once the spout had developed, however, the pressure differences along the base were negligible. On the other hand, results for polyethylene

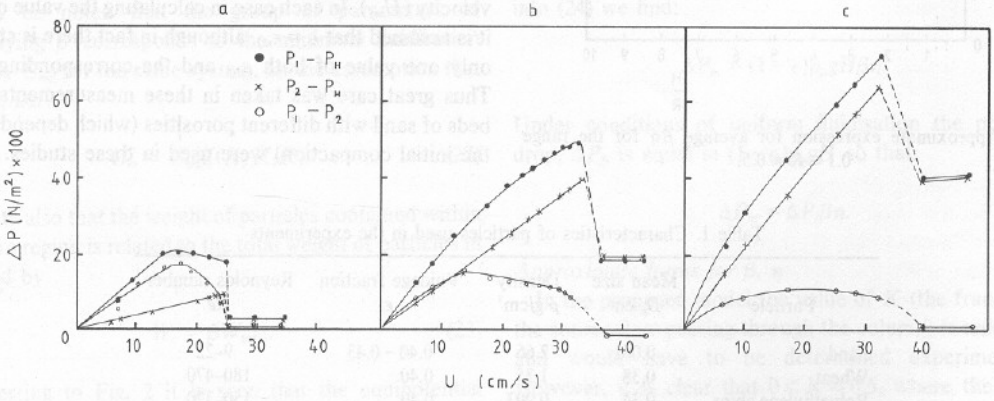

Fig. 8. Pressure drops for a sand bed of $\epsilon = 0.42$; $D_c = 14.2$ cm. (a) $H = 15$ cm; (b) $H = 40$ cm; (c) $H = 59$ cm.

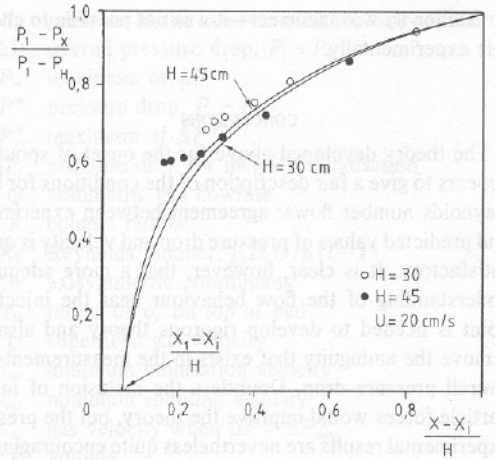

Fig. 9. Measured and computed values for the axial pressure distribution at the centre line for packed bed flow. (Sand, $D_c = 14.2$ cm).

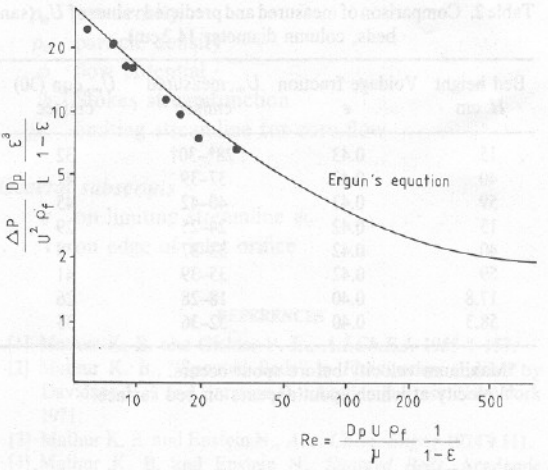

Fig. 11. Measurements of pressure drop vs Reynolds number for uniform flow in the upper portion of sand beds.

particles showed increasingly negative pressure drops along the base with increasing gas velocity, including under spouting conditions. This is shown in Fig. 10. One possible explanation for this is the formation of particle circulation zones close to the bed base, giving lower pressures towards the jet inlet rather than near to the bed wall. A similar phenomenon is also referred to by van Velzen *et al.*[13], who suggest that there may be a venturi-suction effect immediately above the gas inlet.

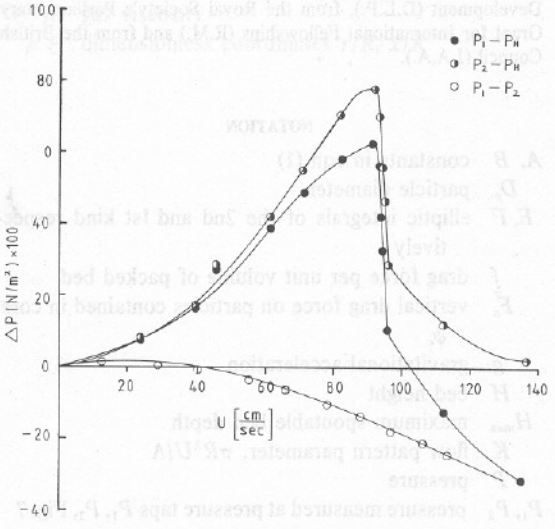

Fig. 10. Pressure drops for a polyethylene bed of $D_c = 14.2$ cm; $H = 27$ cm.

COMPARISON WITH THEORY

The theory developed above assumed low Reynolds number flow in the bed; this was only true for the sand particles ($Re \sim 9$–22), where it was found that a linear relation between pressure drop and velocity did hold for packed beds. Figure 11 shows measurements of pressure drop vs Reynolds number for conditions of uniform flow in the upper portion of the bed in the larger column. Therefore, all comparisons are restricted to this case.

The basic difficulty in comparison lies in the uncertainty surrounding the initial pressure P_i. The evidence of Figs. 8 and 9 indicates that P_i may be considerably higher than any measured value. For the purposes of comparison, in what follows the assumption has been made that the pressure measured as P_1 is the same as that on the equipotential surface intersecting the limiting streamline vertically above the pressure tap P_1 (see Fig. 7). The measured overall pressure drop is thus $\Delta P^* = P_1 - P_H$.

Pressure distribution before the inception of spouting

In Fig. 9 experimental values for the axial pressure distribution are compared with the prediction of the model, computed from eqns (11) and (8) as depicted in Fig. 7, assuming an average value of $K = 0.35$. There is good agreement between experiment and theory for $(x - x_i)/H > 0.25$ and the flow is uniform towards the top of the bed; in the region close to the injector there is a clear deviation from a uniform flow. One reason for the difference between the theory and experiment may lie in the inaccuracy in the model due to the assumptions about the behaviour near the origin: it is assumed that the air jet takes up a concave shape, close to the injection point, but it was impossible to measure the profile in these experiments. A possible interpretation of the trend in the experimental results is that the air "jet" is narrower close to the injector than assumed in the model, which would be consistent with high axial pressure gradients as $x/H \to 0$.

Inception of spouting

(a) *Gas velocity.* As noted above, the transition between packed bed and spouting is very sharp in the case of sand particles. The equilibrium condition thus lies between the maximum velocity before the spout occurs at all and the point at which the spout appears on the bed surface. Experimental values from both these points are compared with theoretical predictions (from eqn 30) in Table 2 for various values of porosity. For $\epsilon = 0.42$ and 0.43 theoretical values are consistently very slightly higher than the experimental values. For $\epsilon = 0.4$ the theoretical values lie within the limits of the experimental

Table 2. Comparison of measured and predicted values of U_m (sand beds, column diameter 14.2 cm)

Bed height H cm	Voidage fraction ϵ	U_m, measured cm/sec	U_m, eqn (30) cm/sec
15	0.43	28*–30†	32
40	0.43	37–39	41
59	0.43	40–42	45
15	0.42	24–25	29
40	0.42	33–37	38
59	0.42	35–39	41
17.8	0.40	18–28	26
58.3	0.40	32–36	35

*Maximum velocity before spout occurs.
†Velocity at which spout appears on bed surface.

values. We conclude that the theory developed above gives a good prediction of the velocities needed for spout formation. The slight deviation may be due to a number of factors including: (a) non-linear ($\Delta P : U$) relations because of the high gas velocities close to the jet; (b) errors due to the extreme sensitivity to voidage fraction (a 2% error in ϵ is equivalent to a relative error of 8% in U_{ms}).

(b) *Maximum pressure drop.* The following new expression for ΔP_m^* was developed using exactly the same procedure that led to eqn (31) for ΔP_m:

$$\Delta P_m^* = \Delta P_f(1 + 0.77\, e^{-0.144H/R}). \qquad (32)$$

Experimental values of the measured maximum pressure drop (ΔP_m^*) are compared with values predicted by eqn (32) in Table 3. The values of $\Delta P_m/\Delta P_m^*$ in this table reflect the difference between P_i and P_1 as discussed earlier. The theoretical values at porosity $\epsilon = 0.42$ are rather higher than the experimental; the agreement between theory and experiments is good for $\epsilon = 0.40$.

The extreme sensitivity of the results to changes in voidage fraction is seen by comparing the third and fifth runs recorded in Table 3. The present theory does not satisfactorily account for this sensitivity. A number of reasons can be considered to explain the deviation from the theoretical. In some cases a slight rearrangement of the bed was noticed before reaching the point of maximum pressure drop; given the sensitivity to the voidage fraction, small changes in bed structure can lead to quite large changes (drops) in overall pressure drop. Secondly, it may well be that the assumption that the base pressure was equal to that on the projection to limiting streamline ψ_c was incorrect—it was not possible to check this experimentally.

CONCLUSIONS

The theory developed above for the onset of spouting appears to give a fair description of the conditions for low Reynolds number flows: agreement between experiment and predicted values of pressure drop and velocity is quite satisfactory. It is clear, however, that a more adequate understanding of the flow behaviour near the injection point is needed to develop rigorous theory and also to remove the ambiguity that exists in the measurements of overall pressure drop. Doubtless the inclusion of inter-particle forces would improve the theory, but the present experimental results are nevertheless quite encouraging.

The experimental results for larger particles also show some significant aspects, and the observations of a reversed flow near the injector are especially interesting. Theory for this situation must include a non-linear relation between pressure drop and velocity and would apparently lead to numerical rather than analytical solutions.

There is a strong incentive to study this regime of operation since particle sizes larger than those for which theory has been developed here are more commonly used in industry.

Acknowledgements—We gratefully acknowledge financial support during part of this work from the Ministry of Overseas Development (D.L.P.), from the Royal Society's Parliamentary Grant for International Fellowships (R.M.) and from the British Council (J.A.A.).

NOTATION

A, B constants in eqn (1)
D_p particle diameter
E, F elliptic integrals of the 2nd and 1st kind respectively
f drag force per unit volume of packed bed
F_x vertical drag force on particles contained in core ψ_c
g gravitational acceleration
H bed height
H_{max} maximum spoutable bed depth
K flow pattern parameter, $\pi R^2 U/\Lambda$
P pressure
P_1, P_2 pressure measured at pressure taps P_1, P_2, Fig. 7

Table 3. Comparison of measured and predicted values of ΔP_m^* (sand beds, column diameter 14.2 cm)

Bed height H cm	Voidage fraction ϵ	$P_1 - P_H$, measured N/m²	ΔP_m^*, eqn(32) N/m²	$\Delta P_m/\Delta P_m^*$, eqns (31) and (32)
15	0.42	2,160	3,540	1.93
40	0.42	4,900	8,120	1.61
59	0.42	7,650	11,020	1.43
17.8	0.40	5,400	4,290	1.88
58.3	0.40	10,800	11,270	1.44

Note: P_1 was not recorded in the first series of experiments with $\epsilon = 0.43$.

P_H pressure at the centreline on top of bed, atm
ΔP overall pressure drop, $P_i - P_H$
ΔP_m maximum of ΔP
ΔP^* pressure drop, $P_1 - P_H$
ΔP_m^* maximum of ΔP^*
ΔP_f pressure drop for incipient fluidisation
Q volumetric gas flowrate
R column radius
Re Reynolds number, $\rho_g D_p U/\mu(1-\epsilon)$
r, x axisymmetric coordinates
r_H radius of ψ_c on top of bed
$U, \underline{U}$ superficial gas velocity
U_{mf} minimum fluidisation velocity
U_{ms} minimum spouting velocity
U_m gas velocity when $\Delta P = \Delta P_{\max}$
V volume
V_c volume within core ψ_c
W_c weight of particles within core ψ_c
W_{total} weight of particles in bed
x_1 axial coordinate of point at centreline where $P = P_1$

Greek symbols

β dimensionless function, defined by eqn (20)
$\bar{\beta}$ mean value of β over range $0.1 < K < 0.5$
η dimensionless function, defined by eqn (25)
$\overline{\beta\eta}$ mean value of $(\beta\eta)$ over range $0.1 < K < 0.5$
ϵ bed voidage fraction
Λ source strength
μ gas viscosity
ρ, ξ dimensionless coordinates r/R, x/R
ρ_g gas density
ρ_p particle density
ϕ flow potential
ψ Stokes streamfunction
ψ_c limiting streamline for core flow

General subscripts

c on limiting streamline ψ_c
i on edge of inlet orifice

REFERENCES

[1] Mathur K. B. and Gishler P. E., *A.I.Ch.E.J.* 1955 **1** 157.
[2] Mathur K. B., "Spouted Beds" in *Fluidization* (Edited by Davidson J. F. and Harrison D.). Academic Press, New York 1971.
[3] Mathur K. B. and Epstein N., *Adv. Chem. Engng* 1974 **9** 111.
[4] Mathur K. B. and Epstein N., *Spouted Beds.* Academic Press, New York 1974.
[5] Madonna L. A. and Lama R. F., *Ind. Engng Chem.* 1960 **52** 169.
[6] Malek M. A. and Lu B. C. Y., *Ind. Engng Chem. Proc. Des. Develop.* 1965 **4** 123.
[7] Volpicelli G. and Raso G., *Atti Accad. Naz. Lincei Rend. Cl. Sci. Fis. Mat. Natur.* 1963 **35** 331.
[8] Manurung F., Ph.D. Thesis, University of New South Wales, Kensington, Australia, 1964 (as quoted in [3, 4]).
[9] Scheidegger A. E., *The Physics of Flow through Porous Media*, 3rd Edn, p. 167. University of Toronto Press 1974.
[10] Robertson J. M., *Hydrodynamics in Theory and Application*, p. 242. Prentice-Hall, Englewood Cliffs, New Jersey 1965.
[11] Asenjo J. A., *Chem. Engng Thesis*, Universidad de Chile, Santiago, Chile 1974.
[12] Lefroy G. A. and Davidson J. F., *Trans. Inst. Chem. Engng* 1969 **47** T120.
[13] van Velzen D., Flamm H. J. and Langenkamp H., *Can. J. Chem. Engng* 1974 **52** 145.